Throughput and Coverage for a Mixed Full and Half Duplex Small Cell Network

Sanjay Goyal *, Carlo Galiotto†, Nicola Marchetti†, and Shivendra Panwar*
*NYU Tandon School of Engineering, Brooklyn, NY, USA
†CONNECT / The Centre for Future Networks and Communications, Trinity College Dublin, Ireland
{sanjay.goyal, panwar}@nyu.edu, {galiotc, marchetn}@tcd.ie

***Abstract*—Recent advances in self-interference cancellation enable radios to transmit and receive on the same frequency at the same time. Such a full duplex radio is being considered as a potential candidate for the next generation of wireless networks due to its ability to increase the spectral efficiency of wireless systems. In this paper, the performance of full duplex radio in small cellular systems is analyzed by assuming full duplex capable base stations and half duplex user equipment. However, using only full duplex base stations increases interference leading to outage. We therefore propose a mixed multi-cell system, composed of full duplex and half duplex cells. A stochastic geometry based model of the proposed mixed system is provided, which allows us to derive the outage and area spectral efficiency of such a system. The effect of full duplex cells on the performance of the mixed system is presented under different network parameter settings. We show that the fraction of cells that have full duplex base stations can be used as a design parameter by the network operator to target an optimal tradeoff between area spectral efficiency and outage in a mixed system.**

***Index Terms*—Full duplex, small cells, stochastic geometry, outage, area spectral efficiency.**

I. Introduction

Recent advances in hardware development [1]–[5] have enabled radios to transmit and receive on the same frequency at the same time, with the potential of doubling the spectral efficiency. Referred to as Full Duplex (FD), these systems are emerging as an attractive solution to the shortage of spectrum for the next generation of wireless networks [6], [7].

Although FD has the capability of enhancing spectral efficiency, simultaneous downlink and uplink operations on the same band generate additional interference, which is likely to erode the performance gain of FD cells [8], [9]. In this work we focus on a mixed multi-cell system, where only some of the base stations (BSs) operate in FD mode, while the remaining BSs are in half duplex (HD) mode [8]–[10]. Using a stochastic geometry-based model that we propose, we investigate the impact of FD cells on the performance of such mixed systems. In particular, we analyze the throughput vs. coverage trade-off of the mixed system as a function of the proportion of FD cells, and for various network parameters such as self-interference cancellation (SIC) levels, and transmit power levels at the BS and at the user equipment (UE).

This work is funded by Higher Education Authority under grant HEA/PRTLI Cycle 5 Strand 2 TGI, Science Foundation Ireland through CONNECT grant number 13/RC/2077, NSF award number 1527750, NYSTAR CATT, and NYU Wireless.

A. Background and related work

To successfully achieve SIC, which is required in order to enable FD operation, the FD circuit has a higher cost and power usage. For this reason, it is more practical to implement FD transmission on the infrastructure devices only, whereas the UE operates in HD mode [9]. An example of this is shown in Fig. 1, where each BS has two UEs scheduled at the same time on the same frequency; one is in uplink, other one is in downlink.

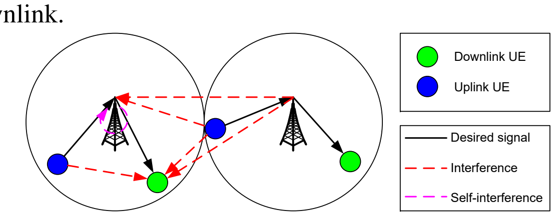

Fig. 1: A full duplex multi-cell interference scenario.

As we can note from Fig. 1, in the uplink, a BS receives interference from UEs transmitting in the uplink as well as from BSs of the neighboring cells transmitting in the downlink. It also receives the residual self-interference, generated by the same BS. In the downlink, a UE receives interference from neighboring BSs as well as from all UEs transmitting in the uplink direction. Thus, during FD operation, each direction receives higher interference compared to the HD case. For example, in a HD synchronized system, where in each timeslot all the cells schedule transmission the same direction, the downlink UE receives interference only from the neighboring BSs, and in the uplink the BS receives interference only from uplink UEs of neighboring cells. As a result of the high interference, FD systems not only cannot achieve their potential spectral efficiency gain, but can suffer from high outage probability.

Mixed multi-cell systems [8]–[10], in which only a given fraction of cells operate in FD mode, have been proposed in order to maintain the interference within a moderate level during FD operations. Although FD cells have the potential of enhancing the area spectral efficiency (ASE) of the network, they also increase the interference, with a consequent drop in terms of coverage.

Among the existing papers addressing FD for wireless networks in multi-cell scenarios, to the best of our knowledge, there is no comprehensive study yet that addresses the ASE vs. coverage trade-off in mixed systems, for both the uplink and the downlink directions. For instance, some works on stochastic geometry for FD operation in wireless networks have been proposed in [10]–[13]. Tong *et al.* [11] investigated the throughput of a wireless network with FD radios using stochastic geometry, but in an ad-hoc setting. Alves *et al.* [12] derived the average spectral efficiency for a dense small cell environment and showed the impact of residual self-interference on the performance of FD operation. Lee *et al.* [10] derives the throughput of a mixed multi-cell heterogenous network consisting of only downlink and/or FD BSs; however, this work only focuses on the downlink, while the uplink performance is not considered. An alternative approach to a multi-cell network with FD operation in each cell is considered in [13], where the authors proposed a scheme which allows a partial overlap between uplink and downlink frequency bands. In [13], it is shown that the amount of the overlap can be optimized to achieve the maximum FD gain. However, all the papers mentioned above: [10], [12], [13] assume the UEs to have FD capabilities, which is neither practical nor economical, given existing FD circuit designs [5]. Moreover, most of the existing work investigates the ASE, while increase in outage probability is not taken into account as a metric to assess the system.

B. Contribution

In this paper, we consider a mixed multi-cell system, in which BSs can operate either in FD or in HD mode, while UEs only operate in HD mode. The main contributions of our work are, (i) we propose a model based on stochastic geometry that allows us to characterize the outage probability and the ASE of both BSs and UEs, for both FD and HD cells; (ii) we investigate the ASE vs. coverage trade-off of mixed systems for different network parameters and we aim at finding the proportion of FD BSs such that some given constraints in terms of ASE or, alternatively, of coverage, can be met.

Among our main findings, we show that the fraction of FD cells can be used as a design parameter to target different ASE vs. coverage trade-offs for the network operator; in particular, by increasing the amount of FD cells in the mixed system, the overall throughput increases at the cost of a drop in terms coverage, and vice-versa.

II. System Model

We consider a network of small cell BSs. The location of BSs and the locations of the UEs are modeled by two independent Spatial Poisson Point Processes (SPPP) Φ_{B} and Φ_{U} with densities λ_{B} and λ_{U}, respectively, where $\lambda_{\mathrm{U}} > \lambda_{\mathrm{B}}$. The BSs are assumed to be capable of FD operation, while the UEs are limited to HD operation. We focus on a single LTE subframe, where all cells are assumed be synchronized in terms of subframe alignment. At any subframe in any cell the BS can either be in FD mode or HD mode. In the case of HD mode the transmission can be either in downlink direction or in uplink direction.

This deployment of BSs will create a Voronoi tessellation with several Voronoi cells, each having nuclei given by the BS locations. We assume that each UE, both in uplink and downlink, is served by the nearest BS. The cumulative distribution function (CDF) of the distance R of the closest BS from a randomly chosen UE is given by:

$$\mathbb{P}\{R \leq x\} = 1 - \exp(-\pi\lambda_B x^2), x \geq 0. \tag{1}$$

Thus the probability density function (PDF) of R is:

$$f_R(x) = e^{-\pi\lambda x^2} 2\pi\lambda x. \tag{2}$$

We further assume that each FD BS will have one uplink UE and one downlink UE scheduled simultaneously at the same subframe whereas each downlink HD BS will have one downlink UE and each uplink HD BS will have one uplink UE active at their subframe. A similar assumption has been made in [14]. We define ρ_{F}, ρ_{D}, and ρ_{U} as the probability of a BS to be in FD mode, downlink HD mode, and uplink HD mode, respectively, with $\rho_{\mathrm{F}} + \rho_{\mathrm{D}} + \rho_{\mathrm{U}} = 1$. By using a thinning process [15, Sec 5.1], the distribution of FD BSs, downlink HD BS, and uplink HD BS also follow independent SPPP $\Phi_{\mathrm{B}}^{\mathrm{F}}$, $\Phi_{\mathrm{B}}^{\mathrm{D}}$, and $\Phi_{\mathrm{B}}^{\mathrm{U}}$, with densities $\rho_{\mathrm{F}}\lambda_{\mathrm{B}}$, $\rho_{\mathrm{D}}\lambda_{\mathrm{B}}$, and $\rho_{\mathrm{U}}\lambda_{\mathrm{B}}$, respectively. Thus, the active downlink UEs served by FD BSs can be described by the SPPP $\Phi_{\mathrm{B}}^{\mathrm{F}}$ with density $\rho_{\mathrm{F}}\lambda_{\mathrm{B}}$; the same model holds for the active uplink UEs served by the FD BSs. Further, the active downlink UEs served by HD BSs can be described by the SPPP $\Phi_{\mathrm{B}}^{\mathrm{D}}$, with density $\rho_{\mathrm{D}}\lambda_{\mathrm{B}}$, and the active uplink UEs served by HD BSs can be described by the SPPP $\Phi_{\mathrm{B}}^{\mathrm{U}}$, with density $\rho_{\mathrm{U}}\lambda_{\mathrm{B}}$.

Note that, the set of interfering UEs and BSs would be correlated due to the association technique mentioned above. However, to maintain model tractability, we assume that the set of interfering UEs is independent of the set of interfering BSs; this assumption has been proved to provide a good approximation for the results in previous works [12], [13].

A. Channel model

In our analysis, we model the different links with different parameters. In general, BSs and UEs are different kinds of nodes in terms of antenna height, antenna characteristics, mobility, etc. For example, different channel models are recommended by 3GPP for BS-to-BS, BS-to-UE, and UE-to-UE links [16]. We considered the following path loss models for the different links that exist in our system:

- BS-to-UE path loss $\mathrm{PL}_1(d) = K_1 d^{-\alpha_1}$.
- UE-to-BS path loss $\mathrm{PL}_1(d) = K_1 d^{-\alpha_1}$.
- UE-to-UE path loss $\mathrm{PL}_2(d) = K_2 d^{-\alpha_2}$.
- BS-to-BS path loss $\mathrm{PL}_3(d) = K_3 d^{-\alpha_3}$.

where α_1, α_2, and α_3 are the path loss exponents; K_1, K_2, and K_3 are the signal attenuations at distance d = 1. We further assume that the propagation is affected by Rayleigh fading, which is exponentially distributed $\sim$ exp(μ) with mean μ^{-1}. In the next subsections, we use g, h, g', and h' to denote Rayleigh fading for the BS-to-UE link, UE-to-UE link, BS-to-BS link, and UE-to-BS link, respectively.

B. BS and UE Transmit Power Allocation

We model downlink transmission with a fixed power transmission scheme. All the BSs transmit with power P_{B}. For uplink modeling, we use distance-proportional fractional power control [17], in which each UE, which is at distance R from its serving BS transmits with power $P_{\mathrm{U}} K_1^{-\epsilon} R^{\epsilon\alpha_1}$, where $\epsilon \in [0,1]$ is the power control factor. If $\epsilon = 1$, the path loss is completely compensated, and if $\epsilon = 0$ all UEs transmit with the same power P_{U}. Both antennas at the BS and at the UE are assumed to be isotropic.

III. SINR Distributions

In this section we present the analytic results for signal to interference and noise ratio (SINR) distributions in our mixed system for both downlink and uplink.

A. Downlink SINR in a FD Cell of the Mixed System

The SINR at a downlink UE of interest in a FD cell of the mixed system, is given by

$$\gamma_{\mathrm{FD,UE}} = \frac{P_{\mathrm{RX,UE}}}{N_0 + I_{\mathrm{D}} + I_{\mathrm{U}}}, \tag{3}$$

where N_0 is the thermal noise power at the downlink UE, and $P_{\mathrm{RX,UE}}$ is the received signal power at the downlink UE from its serving BS, which is given by

$$P_{\mathrm{RX,UE}} = P_{\mathrm{B}} g_{b_0} K_1 r^{-\alpha_1}, \tag{4}$$

where r is the distance between the downlink UE and its serving BS, for which the PDF is defined in (2). The serving BS is indicated by b_0, and g_{b_0} denotes the Rayleigh fading affecting the signal from the BS b_0. I_{D} and I_{U} are the total interference received at the downlink UE from all the downlink transmissions, and from all the uplink transmissions, respectively. The total interference from all the downlink transmissions including all FD cells ($\Phi_{\mathrm{B}}^{\mathrm{F}} \backslash b_0$) and all HD downlink cells ($\Phi_{\mathrm{B}}^{\mathrm{D}}$) can be defined as

$$I_{\mathrm{D}} = P_{\mathrm{B}} \sum_{b \in \{\Phi_{\mathrm{B}}^{\mathrm{D}} \cup \Phi_{\mathrm{B}}^{\mathrm{F}} \backslash b_0\}} g_b K_1 R_b^{-\alpha_1}, \tag{5}$$

where R_b is the distance of the downlink UE from the neighboring active BS b, and g_b denotes the Rayleigh fading for this link. Similarly, I_{U} is the sum of interference from the uplink transmission of FD cells and HD uplink cells,

$$I_{\mathrm{U}} = P_{\mathrm{U}} \sum_{u \in \{\Phi_{\mathrm{B}}^{\mathrm{U}} \cup \Phi_{\mathrm{B}}^{\mathrm{F}}\}} K_1^{-\epsilon} Z_u^{\epsilon\alpha_1} h_u K_2 D_u^{-\alpha_2}, \tag{6}$$

where an uplink UE u, which is at distance Z_u from its serving BS, is transmitting with power $P_{\mathrm{U}} K_1^{-\epsilon} Z_u^{\epsilon\alpha_1}$. It is at distance D_u from the downlink UE of interest, and h_u denotes the Rayleigh fading for the channel between uplink UE u and the downlink UE of interest.

1) Downlink SINR CCDF: In this section we compute the tail distribution or CCDF (complementary CDF) for the downlink SINR. The CCDF of $\gamma_{\mathrm{FD,UE}}$ is computed as:

$$\begin{aligned} \mathrm{P}[\gamma_{\mathrm{FD,UE}} > y] &= \mathbb{E}_r[\mathrm{P}[\gamma_{\mathrm{FD,UE}} > y | r]] \\ &= \int_0^\infty \mathrm{P}[\gamma_{\mathrm{FD,UE}} > y | r = R] f_r(R) \mathrm{d}R. \end{aligned} \tag{7}$$

By using (3) and (4), we can define,

$$\begin{aligned} \mathrm{P}[\gamma_{\mathrm{FD,UE}} > y | r = R] &= \mathrm{P}\left[\frac{P_{\mathrm{B}} g_{b_0} K_1 R^{-\alpha_1}}{N_0 + I_{\mathrm{D}} + I_{\mathrm{U}}} > y\right] \\ &= \mathrm{P}\left[g_{b_0} > y P_{\mathrm{B}}^{-1} K_1^{-1} R^{\alpha_1}(N_0 + I_{\mathrm{D}} + I_{\mathrm{U}})\right] \\ &\overset{(a)}{=} e^{-\mu y P_{\mathrm{B}}^{-1} K_1^{-1} R^{\alpha_1} N_0} \mathcal{L}_{I_{\mathrm{D}}+I_{\mathrm{U}}}(\mu y P_{\mathrm{B}}^{-1} K_1^{-1} R^{\alpha_1}), \end{aligned} \tag{8}$$

where (a) follows from the fact that $g_{b_0} \sim \exp(\mu)$. The Laplace transform of the total interference $(I_{\mathrm{D}}+I_{\mathrm{U}})$, $\mathcal{L}_{I_{\mathrm{D}}+I_{\mathrm{U}}}(s)$, where $s = \mu y P_{\mathrm{B}}^{-1} K_1^{-1} R^{\alpha_1}$, can be written as

$$\begin{aligned} &\mathcal{L}_{I_{\mathrm{D}}+I_{\mathrm{U}}}(s) \\ &= \mathbb{E}_{\Phi_{\mathrm{B}}^{\mathrm{F}} \cup \Phi_{\mathrm{B}}^{\mathrm{D}} \cup \Phi_{\mathrm{B}}^{\mathrm{U}}, g_b, h_u, Z_u}\Big[e^{-s \sum_{b \in \{\Phi_{\mathrm{B}}^{\mathrm{D}} \cup \Phi_{\mathrm{B}}^{\mathrm{F}} \backslash b_0\}} g_b P_{\mathrm{B}} K_1 R_b^{-\alpha_1}} \\ &\times e^{-s \sum_{u \in \{\Phi_{\mathrm{B}}^{\mathrm{U}} \cup \Phi_{\mathrm{B}}^{\mathrm{F}}\}} h_u P_{\mathrm{U}} K_1^{-\epsilon} Z_u^{\epsilon\alpha_1} K_2 D_u^{-\alpha_2})}\Big]. \end{aligned} \tag{9}$$

Using the independence among $\Phi_{\mathrm{B}}^{\mathrm{F}}$, $\Phi_{\mathrm{B}}^{\mathrm{U}}$, and $\Phi_{\mathrm{B}}^{\mathrm{D}}$ mentioned in Section II, we can separate the expectation to obtain:

$$\begin{aligned} \mathcal{L}_{I_{\mathrm{D}}+I_{\mathrm{U}}}(s) = &\underbrace{\mathbb{E}_{\Phi_{\mathrm{B}}^{\mathrm{F}} \cup \Phi_{\mathrm{B}}^{\mathrm{D}}, g_b}\left[e^{-s \sum_{b \in \{\Phi_{\mathrm{B}}^{\mathrm{D}} \cup \Phi_{\mathrm{B}}^{\mathrm{F}} \backslash b_0\}} g_b P_{\mathrm{B}} K_1 R_b^{-\alpha_1}}\right]}_{L_x(s)} \times \\ &\underbrace{\mathbb{E}_{\Phi_{\mathrm{B}}^{\mathrm{F}} \cup \Phi_{\mathrm{B}}^{\mathrm{U}}, h_u, Z_u}\left[e^{-s \sum_{u \in \{\Phi_{\mathrm{B}}^{\mathrm{U}} \cup \Phi_{\mathrm{B}}^{\mathrm{F}}\}} h_u P_{\mathrm{U}} K_1^{-\epsilon} Z_u^{\epsilon\alpha_1} K_2 D_u^{-\alpha_2})}\right]}_{L_y(s)}. \end{aligned} \tag{10}$$

The first term can be further written as

$$\begin{aligned} L_x(s) = &\mathbb{E}_{\Phi_{\mathrm{B}}^{\mathrm{F}}, g_b}\left[e^{-s \sum_{b \in \Phi_{\mathrm{B}}^{\mathrm{F}} \backslash b_0} g_b P_{\mathrm{B}} K_1 R_b^{-\alpha_1}}\right] \\ &\times \mathbb{E}_{\Phi_{\mathrm{B}}^{\mathrm{D}}, g_b}\left[e^{-s \sum_{b \in \Phi_{\mathrm{B}}^{\mathrm{D}}} g_b P_{\mathrm{B}} K_1 R_b^{-\alpha_1}}\right]. \end{aligned} \tag{11}$$

By applying the probability generating functional (PGFL) [15] of the SPPP to (11), it can be further written as:

$$L_x(s) = e^{-2\pi\lambda_{\mathrm{B}}(\rho_{\mathrm{F}}+\rho_{\mathrm{D}}) \int_R^\infty \left(\frac{s K_1 P_{\mathrm{B}} v^{-\alpha_1}}{s K_1 P_{\mathrm{B}} v^{-\alpha_1} + \mu}\right) v \mathrm{d}v}. \tag{12}$$

Similarly the second term in (10) can be written as:

$$\begin{aligned} &L_y(s) = \\ &e^{-2\pi(\rho_{\mathrm{F}}+\rho_{\mathrm{U}})\lambda_{\mathrm{B}} \int_0^\infty \left(1 - \mathbb{E}_{Z_u}\left[\frac{\mu}{s K_2 P_{\mathrm{U}} K_1^{-\epsilon} Z_u^{\epsilon\alpha_1} v^{-\alpha_2} + \mu}\right]\right) v \mathrm{d}v}. \end{aligned} \tag{13}$$

Note that in (12), the lower extreme of integration is R because the closest interferer BS (either FD or HD) from the FD downlink UE of interest is at least at a distance R. However, the closest uplink UE interferer of a FD cell can also be in its own cell, so the lower extreme of integration in (13) is zero. Under the special case of no power control $\epsilon = 0$, expression (13) is converted to:

$$L_y(s) = e^{-2\pi\lambda_{\mathrm{B}}(\rho_{\mathrm{F}}+\rho_{\mathrm{U}}) \int_0^\infty \left(\frac{s K_2 P_{\mathrm{U}} v^{-\alpha_2}}{s K_2 P_{\mathrm{U}} v^{-\alpha_2} + \mu}\right) v \mathrm{d}v}. \tag{14}$$

B. Uplink SINR in a FD Cell of the Mixed System

The SINR for the uplink UE of interest in a FD cell of the mixed system, is given by

$$\gamma_{\mathrm{FD,BS}} = \frac{P_{\mathrm{RX,BS}}}{N_1 + I'_{\mathrm{D}} + I'_{\mathrm{U}} + \mathcal{C}(P_{\mathrm{B}})}, \tag{15}$$

where $P_{\mathrm{RX,BS}}$ is the received signal power from the uplink UE of interest to its serving BS, which is given by

$$P_{\mathrm{RX,BS}} = P_{\mathrm{U}} h'_{u_0} K_1^{(1-\epsilon)} r^{\alpha_1(\epsilon-1)}, \tag{16}$$

where r is the distance between the uplink UE and its serving BS, and h'_{u_0} denotes the Rayleigh fading for this link. In (15), N_1 is the thermal noise power at the BS receiver and $\mathcal{C}(P_{\mathrm{B}})$

is the residual self-interference at the BS, which depends on the transmit power of the BS, P_{B}. We model the residual self-interference as Gaussian noise, the power of which equals the ratio of the transmit power of the BS, P_{B}, and the amount of SIC [9].

In (15), I'_{D} and I'_{U} are the total interference received at the BS from all the downlink transmissions, and from all the uplink transmissions, respectively. These can be defined as

$$I'_{\mathrm{D}} = P_{\mathrm{B}} \sum_{b \in \{\Phi_{\mathrm{B}}^{\mathrm{D}} \cup \Phi_{\mathrm{B}}^{\mathrm{F}} \setminus b_0\}} g'_b K_3 L_b^{-\alpha_3}, \tag{17}$$

$$I'_{\mathrm{U}} = P_{\mathrm{U}} \sum_{u \in \{\Phi_{\mathrm{B}}^{\mathrm{U}} \cup \Phi_{\mathrm{B}}^{\mathrm{F}}\}: X_u > Z_u} h'_u K_1^{(1-\epsilon)} Z_u^{\epsilon\alpha_1} X_u^{-\alpha_1}, \tag{18}$$

where L_b and X_u are the distances of the BS from its neighboring BS b and the active uplink UE u in a neighboring cell, respectively. The constraint $\{X_u > Z_u\}$ in (18) for all $u \in \{\Phi_{\mathrm{B}}^{\mathrm{U}} \cup \Phi_{\mathrm{B}}^{\mathrm{F}}\}$ is from the assumption that each UE is served by its nearest BS.

1) Uplink SINR CCDF: The CCDF for the uplink SINR, $\gamma_{\mathrm{FD,BS}}$, is given by,

$$\mathrm{P}[\gamma_{\mathrm{FD,BS}} > y] = \int_0^\infty \mathrm{P}[\gamma_{\mathrm{FD,BS}} > y | r = R] f_r(R) \mathrm{d}R. \tag{19}$$

By using the similar steps described in section III-A1,

$$\begin{aligned}\mathrm{P}[\gamma_{\mathrm{FD,BS}} > y | r = R] = \; & e^{-\mu y P_{\mathrm{U}}^{-1} K_1^{(\epsilon-1)} R^{\alpha_1(1-\epsilon)} (N_1 + \mathcal{C}(P_{\mathrm{B}}))} \\ & \times \mathcal{L}_{I'_{\mathrm{D}} + I'_{\mathrm{U}}}(\mu y P_{\mathrm{U}}^{-1} K_1^{-1} R^{\alpha_1}),\end{aligned} \tag{20}$$

where the Laplace transform of $(I'_{\mathrm{D}} + I'_{\mathrm{U}})$, assuming $s = \mu y P_{\mathrm{U}}^{-1} K_1^{-1} R^{\alpha_1}$, is given by

$$\begin{aligned}\mathcal{L}_{I'_{\mathrm{D}}+I'_{\mathrm{U}}}(s) = & \underbrace{\mathbb{E}_{\Phi_{\mathrm{B}}^{\mathrm{F}} \cup \Phi_{\mathrm{B}}^{\mathrm{D}}, g'_b}\left[e^{-s \sum_{b \in \{\Phi_{\mathrm{B}}^{\mathrm{D}} \cup \Phi_{\mathrm{B}}^{\mathrm{F}} \setminus b_0\}} g'_b P_{\mathrm{B}} K_3 L_b^{-\alpha_3}}\right]}_{H_x(s)} \times \\ & \underbrace{\mathbb{E}_{\Phi_{\mathrm{B}}^{\mathrm{F}} \cup \Phi_{\mathrm{B}}^{\mathrm{U}}, h'_u, Z_u}\left[e^{-s \sum_{u \in \{\Phi_{\mathrm{B}}^{\mathrm{U}} \cup \Phi_{\mathrm{B}}^{\mathrm{F}}\}: X_u > Z_u} h'_u P_{\mathrm{U}} K_1^{(1-\epsilon)} (\frac{Z_u^\epsilon}{X_u})^{\alpha_1})}\right]}_{H_y(s)}.\end{aligned} \tag{21}$$

The first term in (21) can be further written as,

$$H_x(s) = e^{-2\pi(\rho_{\mathrm{F}} + \rho_{\mathrm{D}})\lambda_{\mathrm{B}} \int_0^\infty \left(\frac{s K_3 P_{\mathrm{B}} v^{-\alpha_3}}{s K_3 P_{\mathrm{B}} v^{-\alpha_3} + \mu}\right) v \mathrm{d}v}. \tag{22}$$

The lower extreme of integration in the above term is zero because the closest interferer BS (either FD or HD) can be at any distance greater than zero. The second term can be further written as:

$$H_y(s) = e^{-2\pi(\rho_{\mathrm{F}} + \rho_{\mathrm{U}})\lambda_{\mathrm{B}} \int_0^\infty \left(1 - \mathbb{E}_{Z_u}\left[\frac{\mu}{s P_{\mathrm{U}} K_1^{1-\epsilon} Z_u^{\epsilon\alpha_1} v^{-\alpha_1} \mathbb{1}\{Z_u < v\} + \mu}\right]\right) v \mathrm{d}v}. \tag{23}$$

The lower extreme of integration in the above term is also zero but the constraint $\{Z_u < v\}$ makes sure that only active UEs from the other cells are included in the interference term. The terms in expression (23) are further solved in Appendix A.

Under the special case of no power control ($\epsilon = 0$), the above expression can be written as:

$$H_y(s) = e^{-2\pi(\rho_{\mathrm{F}} + \rho_{\mathrm{U}})\lambda_{\mathrm{B}} \int_0^\infty \left(\frac{s P_{\mathrm{U}} K_1 v^{-\alpha_1}}{\mu + s P_{\mathrm{U}} K_1 v^{-\alpha_1}}\right) \mathbb{P}(Z_u \le v) v \mathrm{d}v}. \tag{24}$$

C. Downlink and Uplink SINR in the HD Cells of the Mixed System

The downlink SINR at a UE in a HD cell of the mixed system can be derived similarly to the downlink SINR in a FD cell. A downlink UE in a HD cell gets interference from all simultaneous uplink and downlink transmissions similar to the downlink UE in a FD cell. However, there will one difference from the derivation of the SINR CCDF given in Section III-A1. To consider the interference from all the active uplink transmissions, the lower extreme of integration in (13) is zero, which includes the uplink transmission in its own FD cell, whereas in the case of a HD cell, we need to make sure that no uplink transmission inside the downlink UE's own cell is included. For analytical tractability, to take this into account, we make an approximation that the distance from the nearest interfering uplink transmission is approximated by the distance from the nearest interfering BS. This is the same approximation made in [10], [13] while modeling the UE-to-UE interference at a FD UE.

Thus, in this case, the lower extreme of integration in (13) will be R, i.e., the distance of the downlink UE from its serving BS. For this case,

$$L'_y(s) = e^{-2\pi(\rho_{\mathrm{F}} + \rho_{\mathrm{U}})\lambda_{\mathrm{B}} \int_R^\infty \left(1 - \mathbb{E}_{Z_u}\left[\frac{\mu}{s K_2 P_{\mathrm{U}} K_1^{-\epsilon} Z_u^{\epsilon\alpha_1} v^{-\alpha_2} + \mu}\right]\right) v \mathrm{d}v}. \tag{25}$$

Similar to (7), and (8), the expression for CCDF of $\gamma_{\mathrm{HD,UE}}$, is given by,

$$\mathrm{P}[\gamma_{\mathrm{HD,UE}} > y] = \int_0^\infty e^{-\mu y P_{\mathrm{B}}^{-1} K_1^{-1} R^{\alpha_1} N_0} \; L_x(s) \; L'_y(s) f_r(R) \mathrm{d}R, \tag{26}$$

where $s = \mu y P_{\mathrm{B}}^{-1} K_1^{-1} R^{\alpha_1}$.

In the uplink case, the expression for uplink SINR in a HD cell will be given as the uplink SINR in a FD cell in Section III-B but without any self-interference, i.e., $\mathcal{C}(P_{\mathrm{B}}) = 0$,

$$\gamma_{\mathrm{HD,BS}} = \frac{P_{\mathrm{RX,BS}}}{N_1 + I'_{\mathrm{D}} + I'_{\mathrm{U}}}. \tag{27}$$

The CCDF of $\gamma_{\mathrm{HD,BS}}$ is given by,

$$\mathrm{P}[\gamma_{\mathrm{HD,BS}} > y] = \int_0^\infty \mathrm{P}[\gamma_{\mathrm{HD,BS}} > y | r = R] f_r(R) \mathrm{d}R, \tag{28}$$

where

$$\begin{aligned}&\mathrm{P}[\gamma_{\mathrm{HD,BS}} > y | r = R] \\ &= e^{-\mu y P_{\mathrm{U}}^{-1} K_1^{(\epsilon-1)} R^{\alpha_1(1-\epsilon)} N_1} \; \mathcal{L}_{I'_{\mathrm{D}} + I'_{\mathrm{U}}}(\mu y P_{\mathrm{U}}^{-1} K_1^{-1} R^{\alpha_1}),\end{aligned} \tag{29}$$

where, for $s = \mu y P_{\mathrm{U}}^{-1} K_1^{-1} R^{\alpha_1}$, the expression for $\mathcal{L}_{I'_{\mathrm{D}} + I'_{\mathrm{U}}}(s)$ is same as given in (21).

TABLE I: Network Parameters

Parameter	**Value**
Bandwidth	10 MHz
BS Density [nodes/m^2]	10^{-3}
Thermal Noise Density	-174 dBm/Hz
Noise Figure	9 dB (UE), 8 dB (BS)
Path Loss (dB) (R in km) [18]	$140.7 + 36.7\ \log_{10}(R)$
Outage SINR Threshold	-8 dB

IV. Average rate

In general, the average rate per hertz can be computed as follows [17].

$$\mathbb{E}[\mathrm{C}] = \ \mathbb{E}\left[\log_2(1+\gamma)\right] = \int_0^\infty \mathrm{P}\left[\log_2(1+\gamma) > u\right] \mathrm{d}u. \tag{30}$$

By applying this, we can derive the average rate for the downlink and uplink in both FD and HD cells. By using (7) and (8), the average downlink rate in the FD cell is given by

$$\begin{aligned}\mathbb{E}[\mathrm{C}_{\mathrm{FD,UE}}] &= \int_0^\infty \mathrm{P}\left[\log_2(1+\gamma_{FD,UE}) > u\right] \mathrm{d}u \\ &= \int_0^\infty \int_0^\infty e^{-\mu(2^u-1)P_{\mathrm{B}}^{-1}K_1^{-1}R^{\alpha_1}N_0} \times \\ &\mathcal{L}_{I_{\mathrm{D}}+I_{\mathrm{U}}}(\mu(2^u-1)P_{\mathrm{B}}^{-1}K_1^{-1}R^{\alpha_1}) f_r(R)\ \mathrm{d}R\ \mathrm{d}u.\end{aligned} \tag{31}$$

By using (19), and (20), the average uplink rate in a FD cell is given by

$$\begin{aligned}\mathbb{E}[\mathrm{C}_{\mathrm{FD,BS}}] &= \int_0^\infty \mathrm{P}\left[\log_2(1+\gamma_{FD,BS}) > u\right] \mathrm{d}u \\ &= \int_0^\infty \int_0^\infty e^{-\mu(2^u-1)P_{\mathrm{U}}^{-1}K_1^{(\epsilon-1)}R^{\alpha_1(1-\epsilon)}(N_1+\mathcal{C}(P_{\mathrm{B}}))} \times \\ &\mathcal{L}_{I'_{\mathrm{D}}+I'_{\mathrm{U}}}(\mu(2^u-1)P_{\mathrm{U}}^{-1}K_1^{-1}R^{\alpha_1}) f_r(R)\ \mathrm{d}R\ \mathrm{d}u.\end{aligned} \tag{32}$$

Similarly the average downlink and uplink rates in a HD cell, i.e, $\mathrm{E}[\mathrm{C}_{\mathrm{HD,UE}}]$, $\mathrm{E}[\mathrm{C}_{\mathrm{HD,BS}}]$, respectively, can be derived.

Combining the rates of FD and HD cells, the average downlink and uplink rates of the complete network are given by, respectively,

$$\mathbb{E}[\mathrm{C}_{\mathrm{D}}] = \rho_F \mathbb{E}[\mathrm{C}_{\mathrm{FD,UE}}] + \rho_D \mathbb{E}[\mathrm{C}_{\mathrm{HD,UE}}] \tag{33}$$

$$\mathbb{E}[\mathrm{C}_{\mathrm{U}}] = \rho_F \mathbb{E}[\mathrm{C}_{\mathrm{FD,BS}}] + \rho_U \mathbb{E}[\mathrm{C}_{\mathrm{HD,BS}}] \tag{34}$$

V. Numerical Results

In this section, we evaluate the throughput of the proposed mixed system, and present the effect on it of network parameters such as SIC, and the transmit powers of BS and UEs. The performance of the mixed system is also compared with a traditional synchronous TDD half duplex system (THD System), in which, (1) in a given time slot, all cells schedule either uplink or downlink transmission, and (2) the number of time slots is divided equally between the uplink and downlink transmission. In this case, a downlink transmission receives interference from only the neighboring BSs and an uplink transmission receives interference from only the uplink transmissions of the neighboring cells.

Please note that in our analysis in Section III we considered a general model where all the links have different channel parameters and the uplink has power control, however, in this section, we generate results for the specific case of using the same channel parameters for all the different links and with no uplink power control. All uplink UEs transmit with the same power (P_{U}). The effect of different channel parameters for different links and uplink power control will be considered in our future work. We analyze a dense small cell network, for which the network parameter values are described in Table I. With this setting we generate the following numerical results.

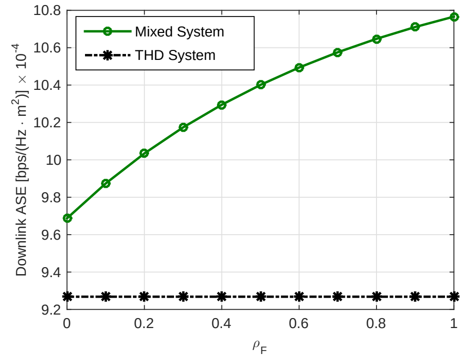

Fig. 2: Downlink ASE as a function of the proportion of FD BSs (ρ_{F}), where $\rho_{\mathrm{D}} = \rho_{\mathrm{U}} = (1-\rho_{\mathrm{F}})/2$. The transmit powers, P_{B} = 24 dBm, P_{U} = 23 dBm. In THD system, $\rho_{\mathrm{D}} = 1$.

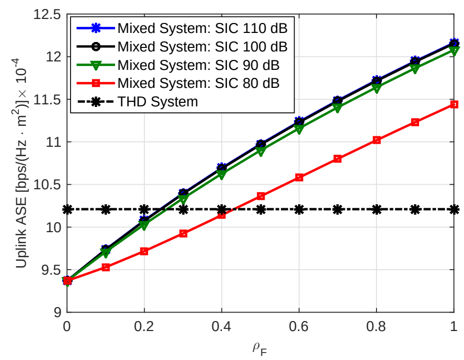

Fig. 3: Uplink ASE as a function of the proportion of FD BSs (ρ_{F}), where $\rho_{\mathrm{D}} = \rho_{\mathrm{U}} = (1-\rho_{\mathrm{F}})/2$. The transmit powers, P_{B} = 24 dBm, P_{U} = 23 dBm. In THD system, $\rho_{\mathrm{U}} = 1$, $\mathcal{C}(P_{\mathrm{B}}) = 0$.

Figs. 2 and 3 show the ASE of the mixed system as a function of the percentage of FD BSs (ρ_{F}) with different SIC. The remaining BSs are equally divided into HD downlink and HD uplink modes, i.e., $\rho_{\mathrm{D}} = \rho_{\mathrm{U}} = (1-\rho_{\mathrm{F}})/2$. The transmit power of the BS and the UE are fixed to 24 dBm, and 23 dBm, respectively.

In the mixed system, as we increase the number of BSs in FD mode, both downlink and uplink ASE increase. As we increase ρ_{F}, both the number of transmissions and the aggregated interference in each direction increase, which generates a tradeoff between ASE and the coverage as shown in Fig. 4. We define coverage as the fraction of UEs in a non-outage region, where an outage happens if the received SINR goes below the outage SINR threshold. The increasing number of transmissions provides higher ASE as shown in Figs. 2 and 3, but a higher outage as well as shown in Fig. 4. The higher ASE gain is therefore achieved at the cost of lower coverage. Thus an appropriate ratio of FD BSs, reflecting a desired optimal

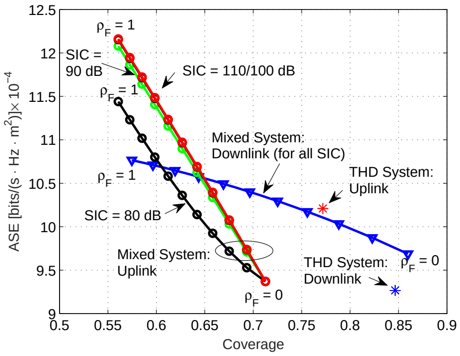

Fig. 4: ASE vs. Coverage, P_{B} = 24 dBm, P_{U} = 23 dBm. For the mixed system, in the downlink, given the coverage of FD cells $\theta_{\mathrm{FD,DL}}$ and of the HD cells $\theta_{\mathrm{HD,DL}}$, the overall downlink coverage of the mixed system is computed as $(\rho_{\mathrm{F}}\theta_{\mathrm{FD,DL}} + \rho_{\mathrm{D}}\theta_{\mathrm{HD,DL}})/(\rho_{\mathrm{F}} + \rho_{\mathrm{D}})$; similarly, the uplink coverage is obtained as $(\rho_{\mathrm{F}}\theta_{\mathrm{FD,UL}} + \rho_{\mathrm{U}}\theta_{\mathrm{HD,UL}})/(\rho_{\mathrm{F}} + \rho_{\mathrm{U}})$.

tradeoff between these two conflicting objectives, should be enabled in the network.

As shown in Fig. 2, the throughput of the downlink direction is not affected by the SIC, because self-interference is received only in the uplink transmission. In the uplink direction, as shown in Fig. 3, the gain of the mixed system increases as SIC improves. It can also noted that there is no improvement in the uplink performance after reducing SIC below 100 dB, because for this dense multi small cell network, after some point inter-cell interference starts dominating the total interference in the uplink direction.

Moreover, Fig. 3 shows that in the uplink direction, the mixed system is superior to THD system when the percentage of BSs in FD mode is higher than 25%-45%, depending on the SIC value, which is not the case in the downlink direction. For lower values of ρ_{F}, in the mixed system most of the cells are in HD mode, similar to the THD system. However, in the mixed system the uplink transmission receives BS-to-BS interference from the cells, which are in HD downlink mode. This interference is generally stronger than the UE-to-BS interference, which decreases the throughput of the mixed uplink system compared to the uplink of THD system, where only UE-to-BS interference exists. However, in the downlink case, UE-to-UE interference is generally weaker than the BS-to-UE interference, which consequently leads to higher throughput in the mixed system even for lower values of ρ_{F}.

Figs. 5 and 6 show the impact of the transmit power of BS (P_{B}) and UE (P_{U}) on the downlink and uplink ASE. In the THD system, downlink performance depends only on P_{B} because the downlink transmission receives interference only from the neighboring downlink transmissions. Similarly, the uplink performance depends only on P_{U}. In the THD system, changing the transmit power does not show much variation in any direction. This is because due to the high density of the BSs, it is an interference limited regime, and changing the transmit power in any direction also proportionately changes the interference, so the SINR does not vary much.

In the mixed system, both downlink and uplink performance depend on the transmit powers of both BS and UE. For the downlink case, as shown in Fig. 5, as we reduce the uplink

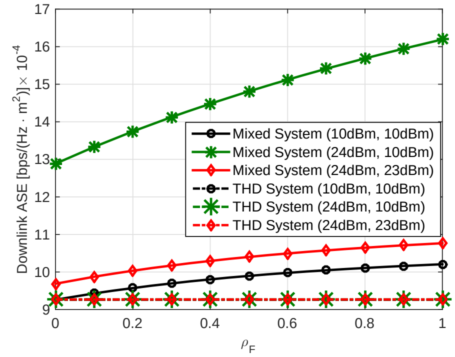

Fig. 5: Downlink ASE as a function of the proportion of FD BSs (ρ_{F}) and with different BS and UE transmit powers ($P_{\mathrm{B}}, P_{\mathrm{U}}$). The other parameters: SIC = 110 dB, $\rho_{\mathrm{D}} = \rho_{\mathrm{U}} = (1 - \rho_{\mathrm{F}})/2$, for THD system, $\rho_{\mathrm{D}} = 1$. Note that all three THD plots overlap completely.

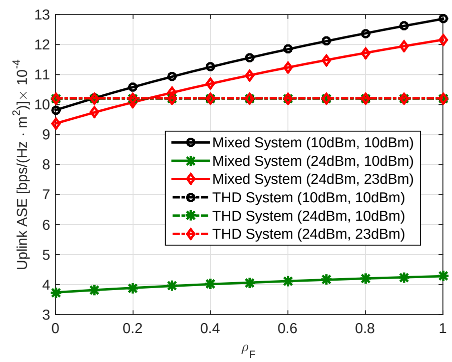

Fig. 6: Uplink ASE as a function of the proportion of FD BSs (ρ_{F}) and with different BS and UE transmit powers ($P_{\mathrm{B}}, P_{\mathrm{U}}$). The other parameters: SIC = 110 dB, $\rho_{\mathrm{D}} = \rho_{\mathrm{U}} = (1 - \rho_{\mathrm{F}})/2$, for THD system, $\rho_{\mathrm{U}} = 1$, $\mathcal{C}(P_{\mathrm{B}}) = 0$. Note that all three THD plots overlap completely.

transmit power, it reduces the UE-to-UE interference, which improves the downlink throughput. The highest downlink gain in all the computed set of transmit powers is achieved when the difference between the downlink and uplink transmit power is maximum, which is the case with P_{B} = 24 dBm, and P_{U} = 10 dBm in Fig. 5. By contrast, in the mixed uplink case, as shown in Fig. 6, the uplink gain improves as the difference between the downlink power and uplink power decreases. For example, in Fig. 6, the highest uplink gain is achieved when the P_{B} is at the same level as P_{U}.

Fig. 7 shows the tradeoff between ASE and coverage for a different set of transmit powers in downlink and uplink. The case of P_{B} = 24 dBm, and P_{U} = 10 dBm provides the highest downlink coverage and downlink ASE but the worst uplink coverage and uplink ASE. These results show the need of an appropriate selection of transmit powers for joint performance gain in the mixed system. In general, to achieve the maximum joint uplink and downlink gain, both uplink and downlink powers should be optimized considering downlink and uplink UEs, as well as a pool of parameters, such as the BS-to-BS, BS-to-UE and UE-to-UE channels, SIC, etc. [8]. In this paper, where we derive average analytical performance using fixed power allocation for all UEs, having similar transmit powers for BS and UE provides a fair performance to both uplink and downlink, while having unbalanced transmit powers benefits one direction at the cost of the other direction which may

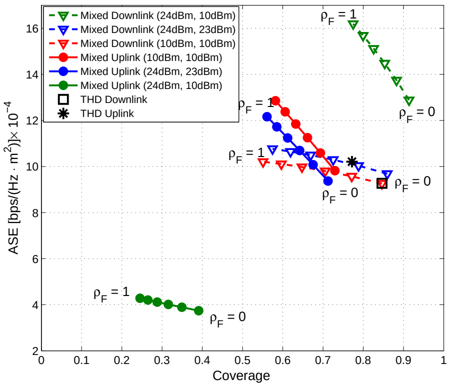

Fig. 7: ASE vs. Coverage with different BS and UE transmit powers ($P_{\mathrm{B}}, P_{\mathrm{U}}$), SIC = 110 dB.

be a desirable outcome if the uplink and downlink traffic is asymmetric.

VI. Conclusion and Future Work

In this paper we considered a mixed multi-cell system, composed of full duplex and half duplex cells, for which we proposed a stochastic geometry-based model that allows us to numerically assess the SINR complementary CDF and the average spectral efficiency, for both the downlink and uplink directions. Using this model, we studied the impact of FD cells on the average spectral efficiency vs. coverage tradeoff of these systems, for various transmit power values at the BS, at the UE, and for different self-interference cancellation levels.

We have shown that increasing the proportion of FD cells increases ASE but reduces coverage and, therefore, can be used as a design parameter of the network to achieve either a better ASE at the cost of limited coverage or a lower ASE with improved coverage, depending on the desired tradeoff between these two performance metrics. Moreover, we show that, in order for the downlink and uplink to achieve similar performance, the transmit power at the BS and at the UE should have similar values, but also that these powers can be tuned to achieve asymmetric uplink and downlink performance improvements if traffic demands dictate this. As future work, we will extend our study to include uplink power control, and to different path loss models for the BS-to-BS, BS-to-UE and UE-to-UE channels.

Appendix A

The integration in (23) can be further solved as

$$\begin{aligned}
&\int_0^\infty \left(1 - \mathbb{E}_{Z_u}\left[\frac{\mu}{sP_{\mathrm{U}}K_1^{1-\epsilon}Z_u^{\epsilon\alpha_1}v^{-\alpha_1}\mathbb{1}\{Z_u < v\} + \mu}\right]\right) v\mathrm{d}v \\
&= \int_0^\infty v\ \mathbb{E}_{Z_u}\left(\frac{1}{\frac{\mu s^{-1}P_{\mathrm{U}}^{-1}K_1^{\epsilon-1}Z_u^{-\epsilon\alpha_1}v^{\alpha_1}}{\mathbb{1}\{Z_u<v\}} + 1}\right) \mathrm{d}v \\
&= \int_0^\infty v \int_0^v \left(\frac{1}{A\ K_1^{\epsilon-1}\ z^{-\epsilon\alpha_1}v^{\alpha_1} + 1}\right) f_{Z_u}(z)\ \mathrm{d}z\ \mathrm{d}v \\
&= G(A, K_1, \epsilon, \alpha_1)
\end{aligned} \tag{35}$$

where $A = \mu s^{-1} P_{\mathrm{U}}^{-1}$. By using integration by parts, $G(A, K_1, \epsilon, \alpha_1)$ can be written as

$$\begin{aligned}
&= \int_0^\infty v \left(\frac{1}{A\ K_1^{\epsilon-1}\ z^{-\epsilon\alpha_1}v^{\alpha_1} + 1}\right) \mathbb{P}\{Z_u \leq z\}\ \mathrm{d}v \\
&- \int_0^\infty v \int_0^v \frac{A\ K_1^{\epsilon-1}\ \epsilon\alpha_1\ z^{-(\epsilon\alpha_1+1)}v^{\alpha_1}}{(A\ K_1^{\epsilon-1}\ z^{-\epsilon\alpha_1}v^{\alpha_1} + 1)^2} \mathbb{P}\{Z_u \leq z\}\ \mathrm{d}z\ \mathrm{d}v
\end{aligned} \tag{36}$$

For $\epsilon = 0$, $G(A, K_1, 0, \alpha_1)$

$$= \int_0^\infty v \left(\frac{1}{A\ K_1^{-1} z^{-\epsilon\alpha_1}v^{\alpha_1} + 1}\right) \mathbb{P}\{Z_u \leq z\}\ \mathrm{d}v \tag{37}$$

References

[1] A. K. Khandani, "Methods for spatial multiplexing of wireless two-way channels," October 2010, US Patent 7,817,641.

[2] M. Knox, "Single antenna full duplex communications using a common carrier," in *Wireless and Microwave Technology Conference (WAMICON), 2012 IEEE 13th Annual*, April 2012, pp. 1–6.

[3] D. Bharadia, E. McMilin, and S. Katti, "Full duplex radios," in *Proceedings of the ACM SIGCOMM 2013*. ACM, 2013, pp. 375–386.

[4] M. Duarte, A. Sabharwal, V. Aggarwal, R. Jana, K. Ramakrishnan, C. Rice, and N. Shankaranarayanan, "Design and characterization of a full-duplex multiantenna system for WiFi networks," *Vehicular Technology, IEEE Transactions on*, vol. 63, no. 3, pp. 1160–1177, March 2014.

[5] A. Sabharwal, P. Schniter, D. Guo, D. Bliss, S. Rangarajan, and R. Wichman, "In-band full-duplex wireless: Challenges and opportunities," *Selected Areas in Communications, IEEE Journal on*, vol. 32, no. 9, pp. 1637–1652, Sept 2014.

[6] Cisco, "Cisco visual network index: Forecast and methodology 2013-2018," Cisco white paper, June 2014. [Online]. Available: www.cisco.com

[7] "NGMN 5G white paper," March 2015. [Online]. Available: www.ngmn.org

[8] S. Goyal, P. Liu, S. Panwar, R. Yang, R. A. DiFazio, and E. Bala, "Full duplex operation for small cells," *CoRR*, vol. abs/1412.8708, 2014. [Online]. Available: http://arxiv.org/abs/1412.8708

[9] S. Goyal, P. Liu, S. Panwar, R. A. Difazio, R. Yang, and E. Bala, "Full duplex cellular systems: Will doubling interference prevent doubling capacity?" *Communications Magazine, IEEE*, vol. 53, no. 5, pp. 121–127, May 2015.

[10] J. Lee and T. Quek, "Hybrid full-/half-duplex system analysis in heterogeneous wireless networks," *Wireless Communications, IEEE Transactions on*, vol. 14, no. 5, pp. 2883–2895, May 2015.

[11] Z. Tong and M. Haenggi, "Throughput analysis for wireless networks with full-duplex radios," in *2015 IEEE Wireless Communications and Networking Conference (WCNC)*, Mar. 2015, pp. 717–722.

[12] H. Alves, C. H. de Lima, P. H. Nardelli, R. Demo Souza, and M. Latva-aho, "On the average spectral efficiency of interference-limited full-duplex networks," in *9th International Conference on Cognitive Radio Oriented Wireless Networks and Communications (CROWNCOM)*. IEEE, 2014, pp. 550–554.

[13] A. AlAmmouri, H. ElSawy, O. Amin, and M. Alouini, "In-band full-duplex communications for cellular networks with partial uplink/downlink overlap," *CoRR*, vol. abs/1508.02909, 2015. [Online]. Available: http://arxiv.org/abs/1508.02909

[14] B. Yu, L. Yang, H. Ishii, and S. Mukherjee, "Dynamic TDD support in macrocell-assisted small cell architecture," *Selected Areas in Communications, IEEE Journal on*, vol. 33, no. 6, pp. 1201–1213, June 2015.

[15] D. Stoyan, W. S. Kendall, J. Mecke, and L. Ruschendorf, *Stochastic geometry and its applications*. Wiley New York, 1987, vol. 2.

[16] 3GPP, "Further enhancements to LTE time division duplex (TDD) for downlink-uplink (DL-UL) interference management and traffic adaptation," TR 36.828, v.11.0.0, June 2012. [Online]. Available: www.3gpp.org

[17] T. D. Novlan, H. S. Dhillon, and J. G. Andrews, "Analytical modeling of uplink cellular networks," *CoRR*, vol. abs/1203.1304, 2012. [Online]. Available: http://arxiv.org/abs/1203.1304

[18] 3rd Generation Partnership Project (3GPP), "Further Advancements for E-UTRA Physical Layer Aspects (Release 9)," Mar. 2010, 3GPP TR 36.814 V9.0.0 (2010-03).